Developmental Cell
Article

The Human Kinetochore Ska1 Complex Facilitates Microtubule Depolymerization-Coupled Motility

Julie P.I. Welburn,[1] Ekaterina L. Grishchuk,[2] Chelsea B. Backer,[1] Elizabeth M. Wilson-Kubalek,[3] John R. Yates III,[3] and Iain M. Cheeseman[1,*]
[1]Whitehead Institute for Biomedical Research and Department of Biology, Massachusetts Institute of Technology, Suite 401, Nine Cambridge Center, Cambridge, MA 02142, USA
[2]Department of Molecular, Cellular, and Developmental Biology, University of Colorado, Boulder, Boulder, CO 80309, USA
[3]Department of Cell Biology, The Scripps Research Institute, La Jolla, CA 92037, USA
*Correspondence: icheese@wi.mit.edu
DOI 10.1016/j.devcel.2009.01.011

SUMMARY

Mitotic chromosome segregation requires that kinetochores attach to microtubule polymers and harness microtubule dynamics to drive chromosome movement. In budding yeast, the Dam1 complex couples kinetochores with microtubule depolymerization. However, a metazoan homolog of the Dam1 complex has not been identified. To identify proteins that play a corresponding role at the vertebrate kinetochore-microtubule interface, we isolated a three subunit human Ska1 complex, including the previously uncharacterized protein Rama1 that localizes to the outer kinetochore and spindle microtubules. Depletion of Ska1 complex subunits severely compromises proper chromosome segregation. Reconstituted Ska1 complex possesses two separable biochemical activities: direct microtubule binding through the Ska1 subunit, and microtubule-stimulated oligomerization imparted by the Rama1 subunit. The full Ska1 complex forms assemblies on microtubules that can facilitate the processive movement of microspheres along depolymerizing microtubules. In total, these results demonstrate a critical role for the Ska1 complex in interacting with dynamic microtubules at the outer kinetochore.

INTRODUCTION

Chromosome segregation during mitosis requires kinetochores to generate physical connections between chromosomes and spindle microtubule polymers. The microtubule interface represents a particular challenge since the kinetochore must not only form contacts with microtubules, but must also remain attached as the microtubules polymerize and depolymerize, as well as couple this growth and shrinkage to chromosome movement. Previous studies have identified a number of components of the kinetochore that form direct connections with microtubules (reviewed in Cheeseman and Desai, 2008; Tanaka and Desai, 2008). The majority of these proteins, such as the plus-end tracking proteins Bim1/EB1, Bik1/CLIP-170, and Stu2/XMAP215; the kinesin-related protein kinesin-8/Kip3, and the multisubunit KNL1/Mis12 complex/Ndc80 complex (KMN) network, are conserved throughout eukaryotes, where they play similar mitotic functions. The combination of these proteins provides the ability to generate stable attachments to microtubule polymers and control the polymerization state of kinetochore-bound microtubules.

In addition to the activities of these conserved outer kinetochore proteins, it is also critical for kinetochores to maintain connections with dynamic microtubule polymers and couple microtubule disassembly to chromosome movement. In budding yeast, this function appears to be provided by the Dam1 complex (also called DASH). The Dam1 complex is a ten subunit microtubule-binding complex (Cheeseman et al., 2001a; Janke et al., 2002; Li et al., 2002) that can form rings (Miranda et al., 2005; Westermann et al., 2005) that encircle and slide along microtubule polymers (Asbury et al., 2006; Grishchuk et al., 2008b; Westermann et al., 2006). However, vertebrate homologs of the Dam1 complex have not been identified. One possibility to explain the absence of a Dam1 homolog is that, in organisms in which multiple microtubules form a dynamic kinetochore bundle, the energy of microtubule depolymerization may be harnessed by using an alternate mechanism (for example, see McIntosh et al., 2008). Alternately, a distinct protein or complex may function to couple kinetochore-microtubule dynamics with chromosome segregation.

To understand the formation of kinetochore-microtubule interactions in vertebrates and the way that these interactions are coupled to microtubule depolymerization, we sought to identify additional components of the human kinetochore-microtubule interface. Recent work identified Ska1 as a component of the human kinetochore (Hanisch et al., 2006). However, the specific role of Ska1 in mediating chromosome segregation was unclear. Here, we demonstrate that the three subunit Ska1 complex is a direct component of the kinetochore-microtubule interface. Importantly, the Ska1 complex displays several key properties that suggest an important role in coupling chromosome movement to microtubule depolymerization, including dual localization to kinetochores and to spindle microtubules during mitosis, a critical role in proper chromosome segregation, a direct microtubule-binding activity, the formation of cooperative oligomeric assemblies on microtubules, and the ability to couple a cargo to the depolymerization of a microtubule polymer.

RESULTS

Purification of a Multisubunit Outer Kinetochore Ska1 Complex

Recent work identified the human kinetochore protein Ska1 (Hanisch et al., 2006). Based on the localization of Ska1 to both kinetochores and microtubules, we hypothesized that it might function at the kinetochore-microtubule interface. To test this, we began by generating stable clonal human cell lines expressing either GFP^{LAP}-tagged Ska1 or Ska2, which has been shown to associate with Ska1 by two-hybrid analysis (Hanisch et al., 2006). Consistent with this previous work, GFP^{LAP}-Ska1 and GFP^{LAP}-Ska2 both localized to kinetochores and spindle microtubules from prometaphase through telophase (Figure 1A). Purification of LAP-tagged Ska1 and Ska2 from these cells isolated a complex containing Ska1, Ska2, and the previously uncharacterized protein Rama1 (also referred to as C13orf3, LOC221150, and Q8IX90.2) (Figure 1B). In Ska1 and Ska2 purifications, we also identified the vesicle trafficking protein SNAP29. However, SNAP29 did not exhibit a similar localization or depletion phenotype to Ska1 (data not shown; Steegmaier et al., 1998), and thus we excluded this protein from further analysis. Less stringent one-step purifications (IPs) with Ska1, but not multistep LAP purifications, additionally isolated small amounts of the spindle checkpoint proteins Bub1 and Bub3 (Figure 1B).

To confirm that Rama1 is a subunit of the Ska1 complex, we generated a cell line stably expressing GFP^{LAP}-Rama1. Similarly to Ska1 and Ska2, GFP^{LAP}-Rama1 localized to kinetochores and microtubules during mitosis, but not during interphase or prophase (Figure 1A). Purification of GFP^{LAP}-tagged Rama1 isolated Ska1 and Ska2, confirming this interaction (Figure 1B). Immunofluorescence with affinity-purified polyclonal antibodies against endogenous Rama1 also revealed kinetochore localization (Figure 1C); however, under the examined fixation conditions, localization to microtubules was not clear. In addition to the kinetochore-associated signal, anti-Rama1 antibodies detected a weak punctuate background staining throughout the cell that is not eliminated by RNAi.

To determine the localization of Rama1 within the kinetochore, we compared the spatial localization of Rama1 relative to the inner kinetochore protein CENP-A and the outer kinetochore protein Ndc80 (Figure 1D). Rama1 precisely colocalized with Ndc80 at the outer kinetochore, and both proteins localized peripherally to CENP-A. Consistent with this localization to the outer kinetochore and prior work on the localization of Ska1 (Hanisch et al., 2006), depletion of the Ndc80 complex subunit Nuf2 abolished the kinetochore localization of Rama1 (Figure 1E). In contrast, depletion of Rama1 eliminated its kinetochore localization, but did not affect localization of hNdc80 (Hec1) to kinetochores (Figure 1E). In total, these results indicate that a three subunit complex containing Ska1, Ska2, and Rama1 localizes to the outer kinetochore and spindle microtubules during mitosis in an Ndc80 complex-dependent manner.

The Ska1 Complex Is Required for Mitotic Chromosome Segregation and Microtubule Organization

To determine the functional roles of the Ska1 complex, we conducted both overexpression and depletion studies. HeLa cells expressing low or moderate amounts of Ska1, Ska2, or Rama1 GFP fusions, either as stable clonal cell lines or using transiently expressed proteins, displayed the mitotic spindle and kinetochore localization described above (Figure 1A). However, in cells transiently overexpressing GFP-Ska1 (Figure 2A), but not Ska2 or Rama1 (not shown), the fusion protein localized to microtubules in interphase cells. In these cases, the microtubules were bundled, suggesting that Ska1 is a microtubule-associated protein that may play a role in microtubule organization.

To examine the function of the Ska1 complex during mitosis and characterize the Rama1 subunit, we depleted Ska1 and Rama1 by RNAi. In both cases, these depletions were effective based on the loss of Rama1 localization to kinetochores (see Figure 2C). Consistent with previous reports (Hanisch et al., 2006), depletion of Ska1 resulted in a mitotic arrest based on fluorescent activated cell sorting (FACS) for DNA content (Figure 2B) and visual examination of the cell population (not shown). Depletion of Rama1 also resulted in a penetrant mitotic arrest (Figure 2B). Codepletion of the mitotic checkpoint component Mad2 eliminated the arrest, indicating that it was a consequence of checkpoint activation (not shown; Hanisch et al., 2006).

Immunofluorescence analysis of Ska1- or Rama1-depleted cells revealed several classes of mitotic defects. In 44% of Ska1-depleted mitotic cells and 36% of Rama1-depleted mitotic cells, the majority of chromosomes were aligned at the metaphase plate, with some off-axis misaligned chromosomes observed (Figure 2C, class 1 phenotype). This is the phenotype that was described previously for depletion of Ska1 and Ska2 (Hanisch et al., 2006). Although we are unable to detect kinetochore-localized Rama1 in these Ska1- or Rama1-depleted cells by immunofluorescence (Figure 2C), this phenotype may reflect incomplete depletion of the Ska1 complex. Other depleted cells displayed much more severe phenotypes, suggesting a critical role for the Ska1 complex in kinetochore-microtubule attachments. About a third of mitotic cells had extensively disorganized chromosomes, reminiscent of depletion of the Ndc80 complex (Figure 2C, class 2 phenotype). The remaining cells displayed highly disorganized chromosomes, but additionally showed an increased number of spindle poles (Figure 2C, class 3 phenotype). Multipolar spindles occurred with a much higher frequency than in control depleted cells (34% versus 4%, for Ska1 depletion and control cells, respectively). In addition, the extra spindle asters appeared to have widely varying sizes and were not evenly situated within the cell, unlike what is observed for the rare multipolar control cells. A similar range of phenotypes were observed after both Ska1 and Rama1 depletion.

The class of phenotypes characterized by multiple spindle poles may reflect a defect in microtubule organization, or a defect in kinetochore function that indirectly causes a change in spindle structure. Given the similarity of the severely misaligned chromosomes to those observed after depletion of the Ndc80 complex, we also depleted the Ndc80 complex subunit Nuf2 by using identical conditions (Figure 2C). In this case, we found that 54% of cells showed multipolar spindles with very similar morphologies to those observed after Ska1 or Rama1 depletion. The multipolar spindles observed after Nuf2 or Rama1 depletion do not appear to result from a failure in cytokinesis during a previous mitosis since the total number of chromosomes in these cells—as assessed by quantitating the number of

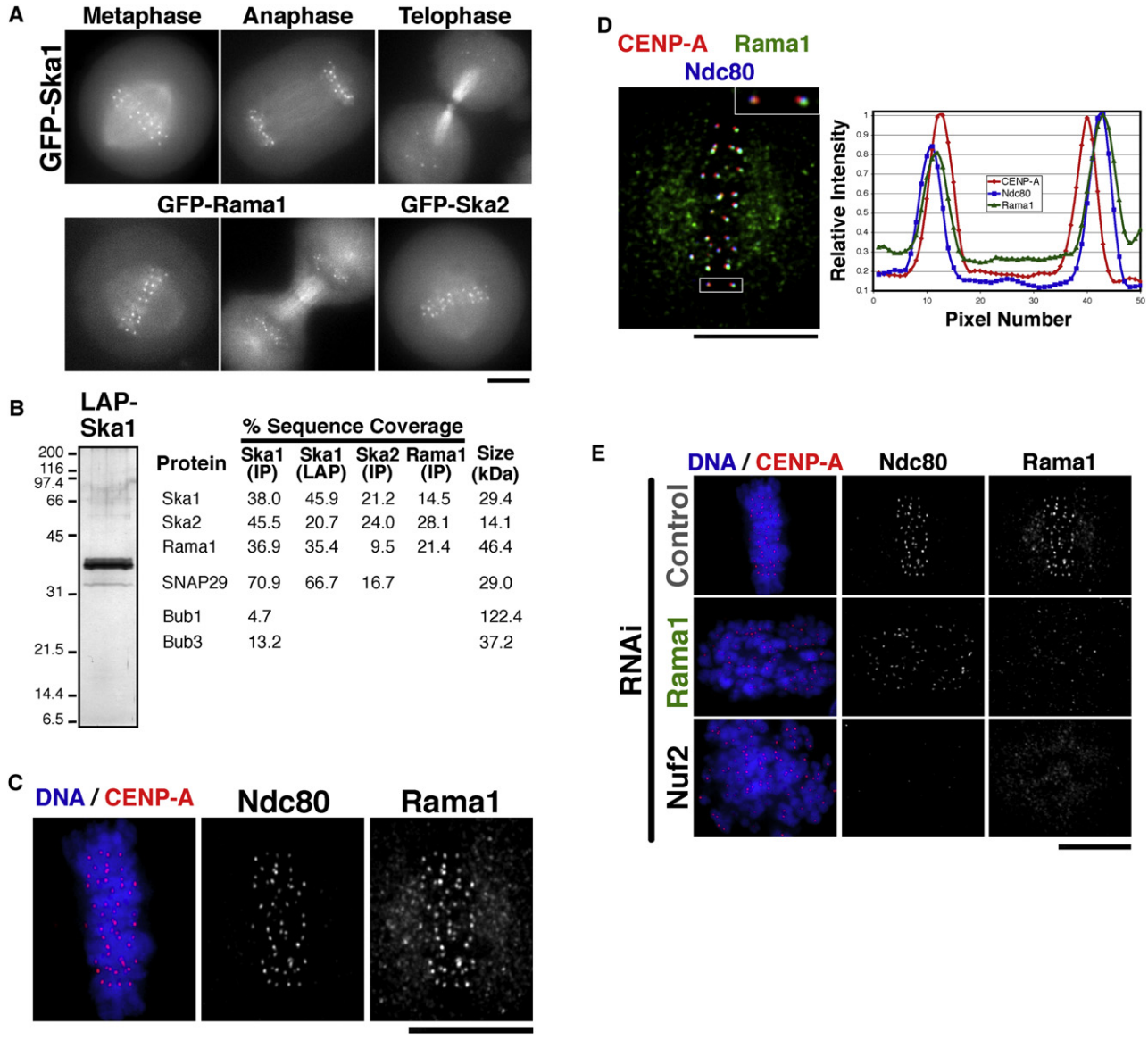

Figure 1. A Three Subunit Human Ska1 Complex Localizes to the Outer Kinetochore and Microtubules

(A) Images of mitotic cells from clonal human cell lines stably expressing moderate amounts of Ska1, Ska2, and Rama1 as GFP^{LAP} fusions. Each fusion protein localizes to kinetochores and microtubules throughout mitosis.

(B) Purification of a three subunit Ska1 complex. GFP^{LAP}-tagged fusions were used to isolate Ska1, Ska2, or Rama1 from the stable cell lines shown in (A) by using either one-step IPs or tandem affinity (LAP) purifications. Left: silver-stained gel of the Ska1 LAP purification. Right: percent sequence coverage from the mass spectrometric analysis of these samples of proteins identified in the Ska1 complex purifications, but not unrelated controls.

(C) Localization of endogenous Rama1. Immunofluorescence with anti-Rama1, anti-HEC1, and anti-GFP (against GFP-CENP-A) antibodies. Rama1 shows a punctuate cellular background staining throughout the cell cycle, but it shows pronounced mitotic localization to kinetochores after nuclear envelope breakdown.

(D) Left: merged image showing colocalization of GFP-CENP-A, Rama1, and HEC1. Right: graph showing a linescan of the fluorescent intensity of the highlighted kinetochore. Rama1 colocalizes with Hec1 at the outer kinetochore and localizes peripherally to CENP-A.

(E) Rama1 kinetochore localization depends on the Ndc80 complex, but the Ndc80 complex localizes to kinetochores independently of Rama1. Immunofluorescence of control cells, Rama1-depleted cells, and Nuf2-depleted cells showing localization of GFP-CENP-A, Ndc80/HEC1, and Rama1.

The scale bars represent 10 μm.

kinetochores—is similar to control cells (data not shown). In addition, only two poles of each multipolar spindle show localization of the centriole marker centrin (see Figure S1 available online). In total, our functional analysis indicates critical roles for the Ska1 complex both in microtubule organization and mitotic chromosome segregation.

Reconstitution of the Ska1 Complex

The dual localization of the Ska1 complex to kinetochores and microtubules, the critical role for the Ska1 complex at the outer kinetochore to mediate proper chromosome segregation, and the defects in microtubule organization observed after overexpression of Ska1 suggested the possibility that this complex

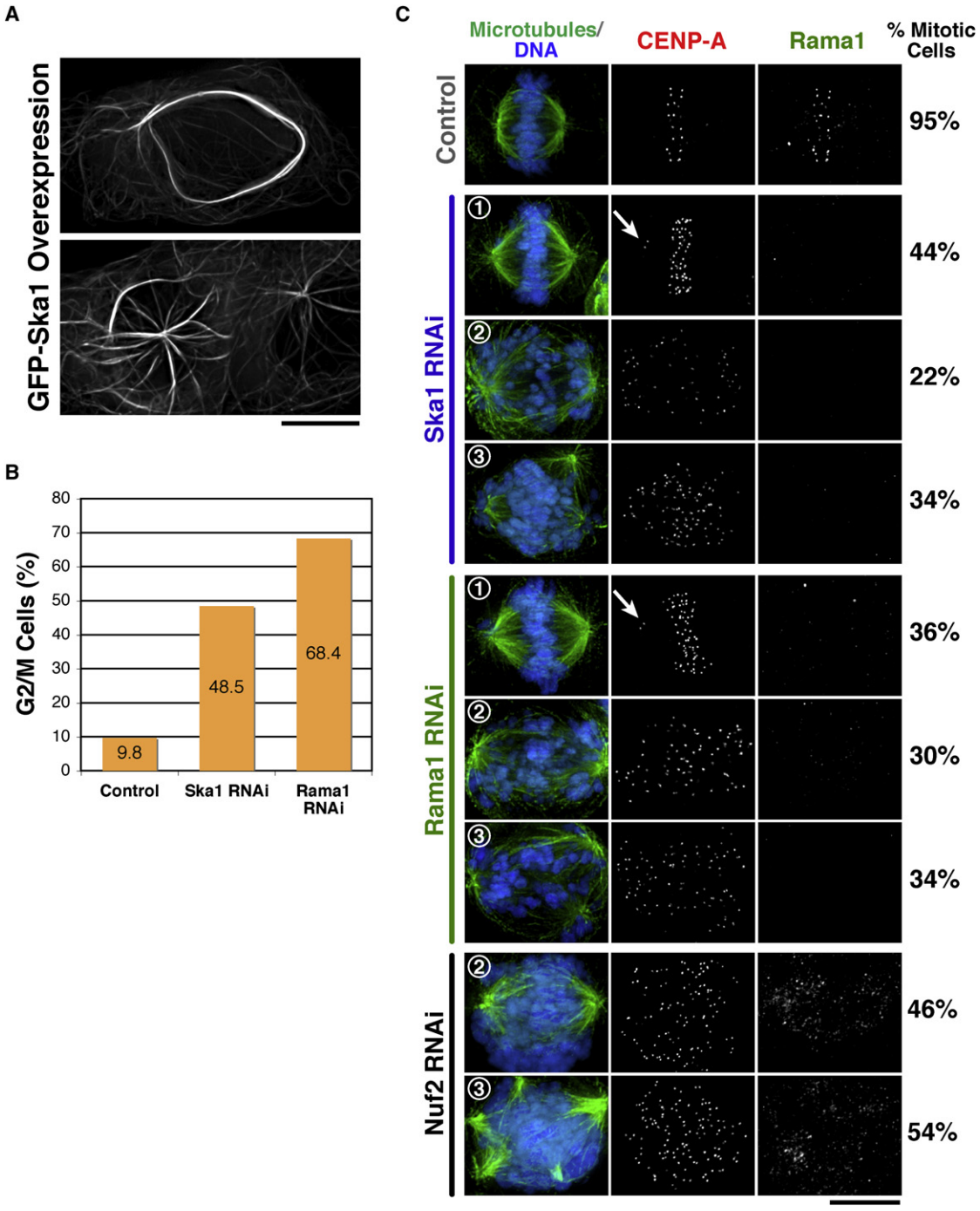

Figure 2. The Ska1 Complex Is Required for Kinetochore-Microtubule Attachments

(A) Overexpression of GFP-Ska1 results in the localization to, and bundling of, interphase microtubules. HeLa cells were transiently transfected with a GFP-Ska1 plasmid and imaged 32 hr after transfection.

(B) Depletion of Ska1 or Rama1 results in a penetrant mitotic arrest. The graph shows the percentage of G2/M cells based on the fluorescent-activated cell sorting and staining against DNA. Visual examination of these cells confirmed that they were arresting in mitosis (not shown).

(C) Depletion of Ska1 and Rama1 results in severe chromosome segregation defects. Depleted cells were imaged for microtubules (by using anti-tubulin antibodies), DNA, CENP-A (by using anti-GFP antibodies in a cell line stably expressing GFP-CENP-A), and Rama1 (by using anti-Rama1 antibodies). (1) Class 1 phenotype with the majority of chromosomes aligned at the metaphase plate. Arrows point to a single pair of off-axis chromosomes in the depleted cells. (2) Class 2 phenotype with chromosomes severely misaligned. (3) Class 3 phenotype with misaligned chromosomes and multipolar spindles. For each condition, 600 mitotic cells were counted to quantify the percentage of cells with each of the indicated phenotypes.

Scale bars represent 10 μm.

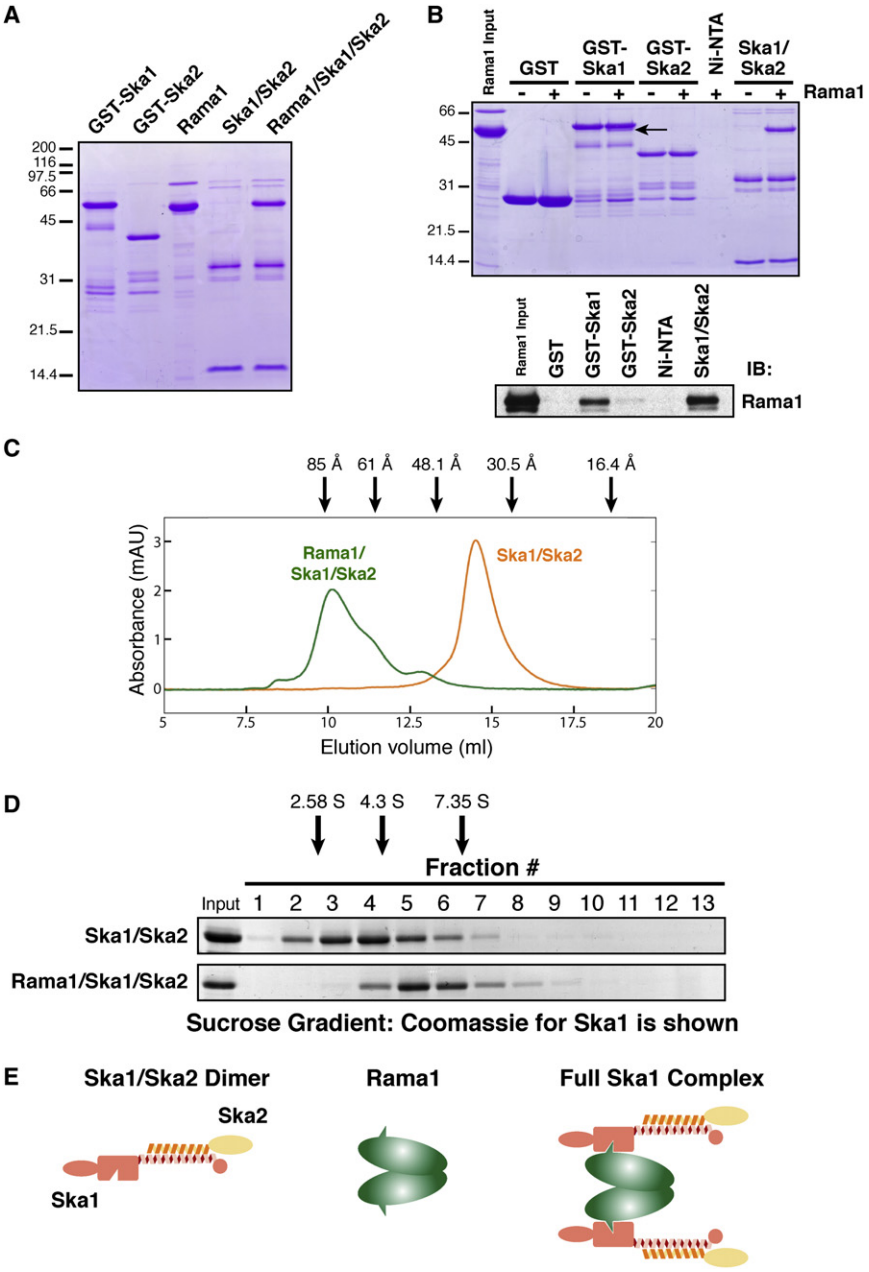

Figure 3. Reconstitution of the Human Ska1 Complex

(A) Coomassie-stained gel showing purified GST-Ska1, GST-Ska2, untagged Rama1 (isolated as a GST fusion and cleaved with PreScission protease), a Ska1/Ska2 dimer (isolated with a 6xHis-tagged Ska1), and a three subunit Rama1/Ska1/Ska2 complex (isolated by mixing the Rama1 subunit with the Ska1/Ska2 dimer).

(B) Rama1 binds to the Ska1 complex through the Ska1 subunit. Top: Coomassie-stained gel showing a resin-based binding assay for Rama1 to either glutathione agarose beads containing GST (as a control), GST-Ska1, or GST-Ska2, or Ni-NTA agarose beads alone (as a control), or containing the Ska1/Ska2 dimer. Rama1 (arrow) runs at a similar size to GST-Ska1 on SDS-PAGE gels. Bottom: western blot to visualize Rama1 in these binding assays. The western blot confirms the binding to GST-Ska1, but not to GST-Ska2.

(C) Graph showing the elution profile of the full Rama1/Ska1/Ska2 complex or the Ska1/Ska2 dimer on a Superdex 200 size-exclusion column (based on OD_{280} absorbance). Arrows indicate the migration of standards with known Stokes radii: Thyroglobulin (85 Å), Ferritin (61 Å), Aldolase (48 Å), and Ovalbumin (30.5 Å).

(D) Coomassie-stained gel showing the profile of the full Rama1/Ska1/Ska2 complex or the Ska1/Ska2 dimer in a 5%–20% sucrose gradient. Arrows indicate the migration of standards with known S values: Chymotrypsinogen A (2.58 S), BSA (4.3 S), and Aldolase (6.5 S).

(E) Diagram showing the organization of the Ska1 complex based on the reconstitution experiments in this figure.

associates directly with microtubule polymers. To test this, as well as analyze the organization of the Ska1 complex, we expressed its subunits either individually or in combination in bacteria. We purified GST-Ska1, GST-Ska2, and Rama1 individually from bacteria (Figure 3A). In addition, we purified a dimer of Ska1-6xHis and untagged Ska2 by coexpressing these proteins (Figure 3A). Resin-based binding assays demonstrated that Rama1 directly associates with GST-Ska1 and the Ska1-6xHis/Ska2 dimer, but not to GST-Ska2 alone (Figure 3B). Finally, we were able to reconstitute the full Rama1/Ska1/Ska2 complex by combining purified Rama1 with purified Ska1/Ska2 and then conducting gel-filtration chromatography (Figure 3A). The reconstituted Ska1 complex contains approximately equimolar amounts of Ska1, Rama1, and Ska2 based on the relative intensities of these proteins in Coomassie-stained gels (Figure 3A; data not shown). We will refer to this Rama1/Ska1/Ska2 complex as the full Ska1 complex.

To determine the size and shape of the Ska1 complex, we analyzed the reconstituted proteins by gel filtration and sucrose gradients. Based on comparison to standards, analysis of the full Ska1 complex and the Ska1/Ska2 dimer by gel filtration indicated Stokes radii of 78 and 44 Å, respectively (Figure 3C). Similarly, the sucrose gradient analysis indicated S values of 5.7 and 3.2 for the full Ska1 complex and the Ska1/Ska2 dimer, respectively (Figure 3D). Calculations with the Stokes radii and the S values of these complexes (see Siegel and Monty, 1966) suggest native molecular weights of 184 kDa for the full Ska1 complex and 56 kDa for the Ska1/Ska2 dimer. The Ska1/Ska2 dimer has a predicted molecular weight of 43.7 kDa, suggesting that this minimal complex contains a single molecule of each subunit. In contrast, the full Ska1 complex has a combined predicted molecular weight of 90 kDa, suggesting that the native complex contains two molecules of each subunit. In addition to defining the molecular organization (diagrammed in Figure 3E), the Stokes radii determined for these complexes indicate elongated shapes.

For comparison, aldolase has a similar Stokes radius to the Ska1/Ska2 dimer (48 Å), but a molecular weight that is three times larger (161 kDa versus 56 kDa), whereas thyroglobulin has a Stokes radius similar to that of the full Ska1 complex (85 Å), but a molecular weight that is greater than three times larger (650 kDa versus 184 kDa). In total, these studies defined the organization of the Ska1 complex and provide reconstituted protein for the biochemical studies described below.

The Ska1 Complex Binds Directly to Microtubules

To test the binding of the reconstituted Ska1 complex to microtubules, we conducted microtubule cosedimentation assays by using limiting protein concentrations of the individually reconstituted Ska1 complex subunits (50 nM; Figure 4A). None of the subunits sedimented in the absence of microtubules. However, GST-Ska1 cosedimented with microtubules in a concentration-dependent manner. GST-Ska2 also bound directly to microtubules, albeit at very low levels. In contrast, Rama1 did not bind directly to microtubules on its own.

To determine the microtubule-binding affinity of the Ska1 complex, we varied the microtubule concentration and determined the concentration required for half maximal binding (Figures 4B and 4C), which corresponds to the apparent microtubule-binding affinity. The Ska1/Ska2 dimer bound to microtubules with an apparent affinity of ~0.6 μM. Although Rama1 did not bind directly to microtubules on its own, it was able to cosediment with microtubules when present in the full Ska1 complex. Addition of the Rama1 subunit resulted in a slight increase in the overall microtubule-binding affinity to ~0.3 μM. The microtubule-binding affinity of the full Ska1 complex is comparable to that of the Dam1 complex and the KMN network, both of which bind to microtubules with an apparent affinity of ~0.5 μM (Cheeseman et al., 2001a, 2006).

We next examined the microtubule-binding properties of the Ska1 complex in greater detail. Previous work has shown that a number of microtubule-binding proteins, including the Dam1 complex (Westermann et al., 2005) and the Ndc80 complex (Wilson-Kubalek et al., 2008), associate with microtubules through the acidic C terminus of tubulin. To determine whether the Ska1 complex shows a similar mode of microtubule binding, we treated polymerized microtubules with the protease subtilisin to remove the tubulin C terminus. These experiments indicated a significant reduction in binding activity upon cleavage of the acidic C terminus (Figure 4D), indicating a similar mode of binding to known microtubule-associated proteins.

Next, we determined the stoichiometry of binding of the Ska1 complex to microtubules. For these experiments, we used saturating amounts of Ska1 complex in the presence of 0.5 μM microtubules. Analysis of Coomassie-stained gels of the pellet fractions of these reactions indicated a ratio of ~1 Ska1/Ska2 dimer or full Ska1 complex bound per tubulin dimer in the microtubule (Figure 4E). In total, these results demonstrate that the Ska1 complex binds directly to microtubules through the Ska1 subunit with properties consistent with established microtubule-binding components of the kinetochore.

The Ska1 Complex Binds Cooperatively to Microtubules

The results described above indicate that the Ska1 complex directly associates with microtubule polymers. There are several ways in which such an interaction can occur. First, the Ska1 complex may function as an individual, independent unit to facilitate kinetochore-microtubule interactions. Second, the Ska1 complex may form an oligomeric assembly on microtubules. An oligomeric assembly requires interactions between neighboring Ska1 complexes on the microtubule and would likely be reflected as cooperative binding in the cosedimentation assay. Thus, in addition to examining the microtubule-binding behavior of the Ska1 complex at a fixed, limiting concentration, we also examined the concentration dependence of the microtubule-binding activity. Small changes in the input concentration of the Ska1 complex resulted in dramatic changes in the apparent microtubule-binding activity (Figure 4F), reaching a maximal binding affinity of ~0.2 μM at 100 nM protein. We also examined the microtubule-binding activity of a range of concentrations of both the Ska1 complex and the Ska1/Ska2 dimer in the presence of excess (5 μM) microtubules. The Ska1/Ska2 dimer displayed a minor concentration-dependent increase in microtubule binding (Figure 4G). This change was similar to the Ndc80 complex, which does not show strong cooperativity at the concentrations shown in Figure 4G (also see Cheeseman et al., 2006). In contrast, the complete Ska1 complex displayed strongly cooperative microtubule-binding activity (Figure 4G). These results indicate that the microtubule-binding activity of the Ska1/Ska2 dimer is not cooperative on its own; however, in the presence of the Rama1 subunit, the full Ska1 complex shows a highly cooperative microtubule-binding behavior.

Our previous work on the Ndc80 complex revealed a cooperative microtubule binding-behavior at higher input concentrations (Cheeseman et al., 2006). In the case of the Ndc80 complex, one explanation for this cooperative behavior is the microtubule bundling that is observed at high concentrations. To determine whether this was the case for the Ska1 complex, we examined its microtubule-bundling activity. We found that high concentrations of the Ska1 complex bundled microtubule polymers (Figure 4H). However, we did not observe bundling at lower concentrations at which cooperative microtubule binding was observed in the cosedimentation assays. In addition, the Ska1/Ska2 dimer displayed microtubule-bundling activity at a similar range of concentrations (not shown), but did not show cooperative microtubule binding (Figure 4G). In total, these experiments demonstrate that the Ska1 complex binds directly to microtubules and displays a cooperative microtubule-binding activity. This latter activity suggests self-association of Ska1 complex molecules on the same microtubule.

The Ska1 Complex Forms Oligomeric Assemblies on Microtubules

The cooperative binding activity that we identified and described above suggested that the Ska1 complex may interact with itself in the presence of microtubules. To examine the presence of oligomeric Ska1 complex structures on microtubules, and to directly visualize the association of the Ska1 complex with microtubules, we next imaged the full Ska1 complex bound to microtubule polymers by negative-stain electron microscopy (EM). The Ska1 complex showed a decoration of the microtubules that is consistent with the formation of oligomeric assemblies (Figure 5). The cooperative behavior of the Ska1 complex was also observed by EM. Although some microtubules were fully decorated, other

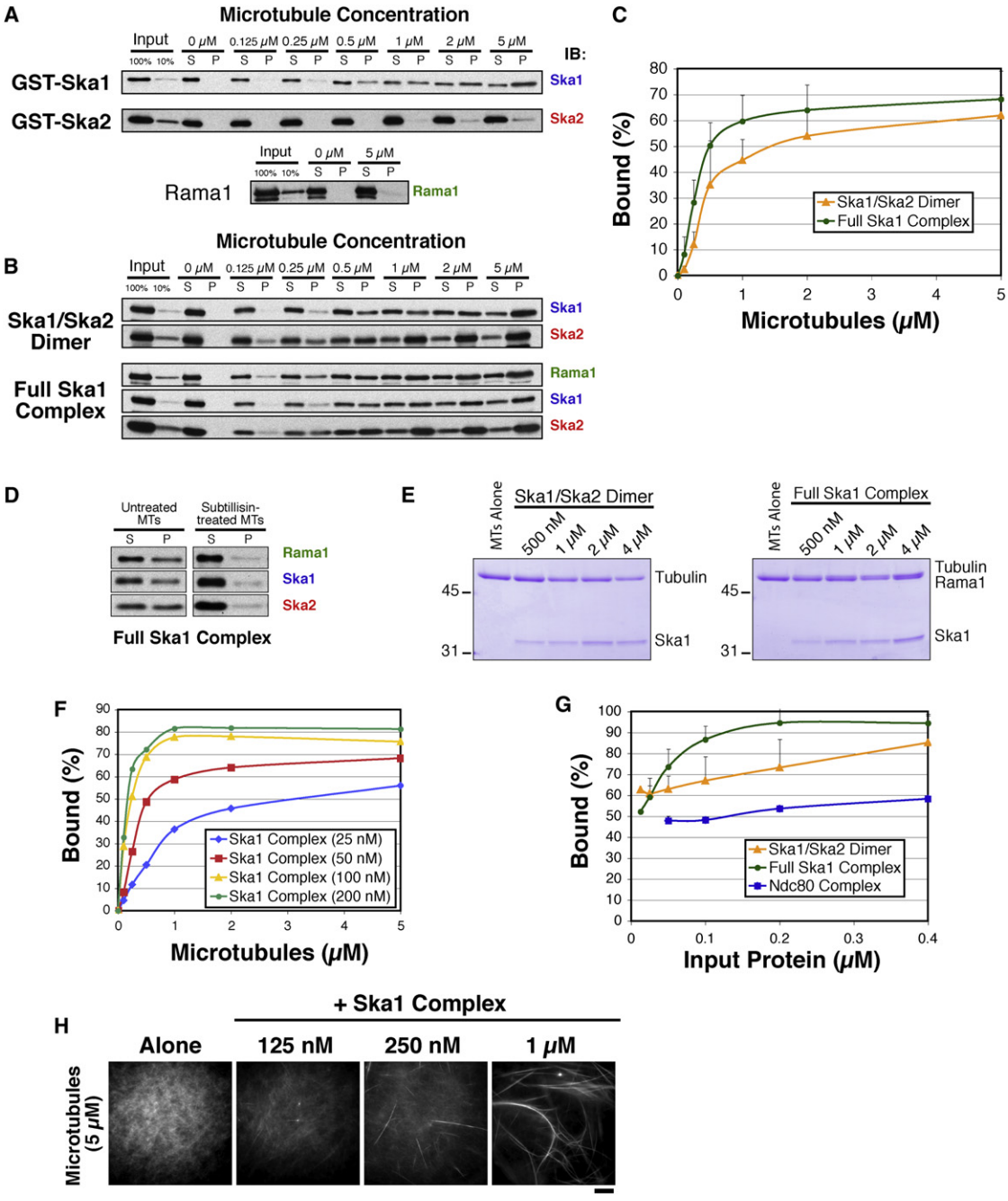

Figure 4. The Ska1 Complex Binds Cooperatively to Microtubules In Vitro

(A) Western blot with the indicated antibodies showing the cosedimentation of 50 nM GST-Ska1, GST-Ska2, or Rama1 with microtubules at the indicated concentrations of polymerized tubulin. At least two samples were examined for each protein.

(B) Cosedimentation of the Ska1/Ska2 dimer, or the full Ska1 complex as in (A) with 50 nM input protein.

(C) Graph plotting the quantification of the microtubule-binding data shown in (B). The average of multiple samples were plotted for Ska1/Ska2 (n = 3) and Rama1/Ska1/Ska2 (n = 7). Error bars indicate standard deviation.

(D) Binding of the Ska1 complex to microtubules requires the acidic C terminus of tubulin. Treatment of GMPCPP microtubules with subtilisin greatly reduces the binding of the Ska1/Ska2/Rama1 complex based on a western blot of a microtubule cosedimentation assay relative to untreated microtubules.

(E) Stoichiometry of microtubule binding. Coomassie-stained gels showing the pellet fractions containing 0.5 μM microtubules and the indicated concentrations of the Ska1/Ska2 dimer or the full Ska1 complex. Rama1 runs at the same molecular weight as tubulin in SDS-PAGE gels.

(F) The Ska1 complex shows cooperative microtubule-binding behavior. A graph showing microtubule binding as in (C), but with a range of protein input concentrations.

(G) A graph showing the binding of the indicated concentrations of the Ska1/Ska2 dimer, the Ska1 complex, or the Ndc80 complex with 5 μM microtubules. Error bars indicate standard deviation.

(H) The Ska1 complex bundles microtubules in vitro. Fluorescent images showing rhodamine-labeled microtubules in the presence of the indicated concentrations of the Ska1 complex. The scale bar represents 10 μm.

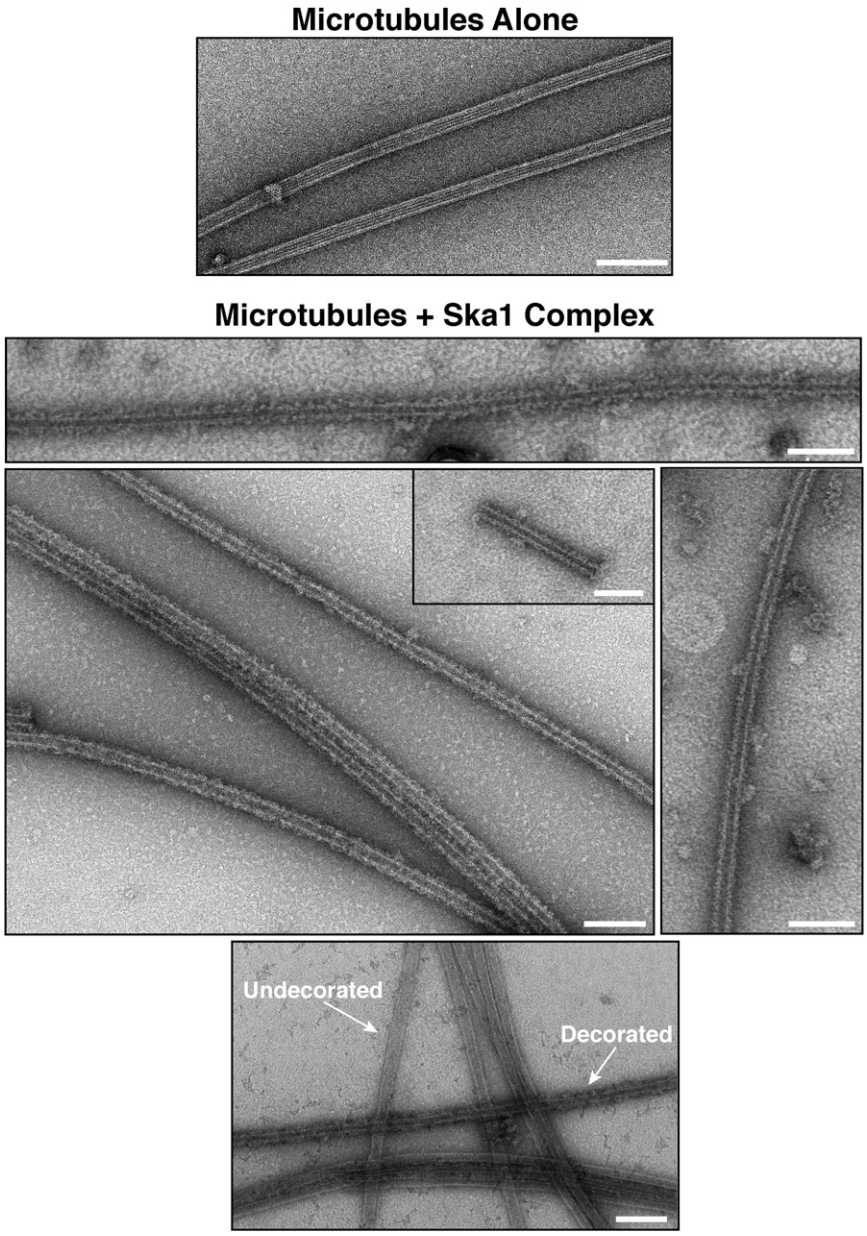

Figure 5. The Ska1 Complex Forms Ring-like Assemblies on Microtubules

Electron microscopy of negatively stained taxol-stabilized microtubules either alone or with Ska1 complex bound. In the bottom image, microtubules with Ska1 complex bound and undecorated microtubules are visible in the same field (indicated by arrows). The scale bars represent 100 nm.

microtubules in the same field remain unbound (Figure 5, bottom image). Together with the cosedimentation assays, these results demonstrate a microtubule-dependent oligomerization of the Ska1 complex to generate assemblies on microtubules.

The Ska1 Complex Can Couple a Cargo to Microtubule Depolymerization

The above-described results strongly suggest that the Ska1 complex plays a direct role in mediating kinetochore-microtubule interactions. Given the oligomeric assemblies that this complex forms on microtubules, we next sought to determine the ability of the Ska1 complex to mediate the association of a cargo with a depolymerizing microtubule end. To test if the Ska1/Ska2 dimer or the full Ska1 complex can couple microtubule depolymerization to cargo motion, we used 0.5 μm microspheres coated with the corresponding complexes and additionally added 2.5–6 nM soluble protein (see Experimental Procedures). The beads were allowed to bind to microtubule polymers that were grown from coverslip-bound *Chlamydomonas* axonemes (Figure 6A). Microtubules were induced to depolymerize (Grishchuk et al., 2005), and we recorded bead motions by using DIC microscopy (Figure 6B; Movies S1 and S2). A considerable fraction of these beads displayed depolymerization-directed movement (Figure 6C). The average run length for the Ska1/Ska2 dimer and the full Ska1 complex beads was 2 and 3.5 μm, respectively (Figure 6E), indicating significant processivity. Thus, both the minimal Ska1/Ska2 dimer and the full Ska1 complex can robustly support motion of a bead cargo with a shortening microtubule end. Although the full Ska1 complex initiates fewer bead motions (Figure 6C), the Rama1 subunit promoted an increased processivity to the movement (Figure 6D).

Previous studies of Dam1 complex-mediated motility have revealed two distinct modes of motion of the Dam1 complex-coated beads (Grishchuk et al., 2008b). Dam1-coated beads can be transported by the shortening microtubule end even in the absence of soluble Dam1, which precludes formation of the microsphere-associated ring-like structures. Under these conditions, the beads move faster than the standard rate of microtubule disassembly, presumably because the bending of the shortening microtubule protofilaments is enhanced by the rolling bead motions. In contrast, under conditions in which rings of the Dam1 complex are formed, the beads move significantly slower than the normal rate of microtubule depolymerization due to the bead-associated Dam1 ring impeding microtubule disassembly (Grishchuk et al., 2008a). To gain insight into the mechanism of the bead motions supported by the Ska1/Ska2 dimer and the full Ska1 complex, we measured their rates by determining the slopes of the linear fits in distance versus time plots (Figure 6E). Based on this quantification, the rate of motion of Ska1/Ska2 dimer-coated beads varied significantly (Figures 6F and 6G), with the mean rate similar to the average rate of free microtubule disassembly ~25 μm/min). In

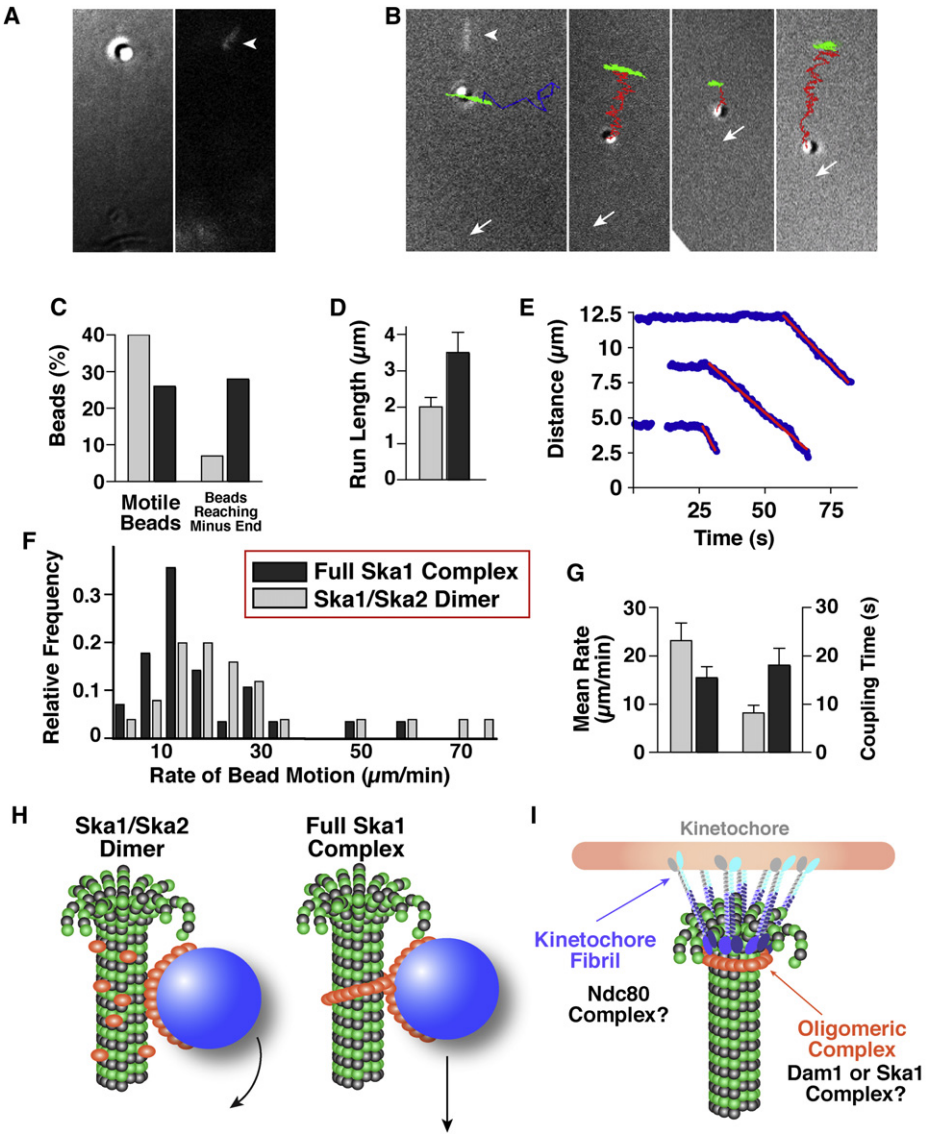

Figure 6. The Ska1 Complex-Coated Microspheres Display Microtubule Depolymerization-Driven Motility

(A) DIC image (left panel) of a microtubule-bound bead with a corresponding fluorescent image (right panel) showing the stabilized microtubule cap (arrowhead).

(B) Example trajectories of moving Ska1 complex-coated beads overlayed with the terminal corresponding DIC image. The trajectory of a bead that is stably attached to the wall of a static microtubule polymer (green) resembles a short arc, because the unattached microtubule plus end swings randomly as the overall microtubule length remains constant. Bead detachment from a microtubule is evidenced by a change of this swinging motion into a random "walk" (blue trajectory). Microtubule depolymerization-driven bead motions (red trajectories) are linearly directed, and the amplitude of their swinging motions diminishes as the microtubule shortens. Arrows indicate positions of the coverslip-attached microtubule minus ends. The first panel additionally shows an overlayed fluorescent image of the rhodamine-labeled microtubule cap before photoablation (arrowhead).

(C) A graph showing the percentage of beads that moved > 0.5 μm, and the percentage of moving beads that reached the microtubule end (full Ska1 complex, n = 112; Ska1/Ska2 dimer, n = 68).

(D) A graph showing the mean distances traveled (± standard error of the mean [SEM]) for the Ska1 complex and Ska1/Ska2 dimer-coated beads.

(E) A graph showing the relative distance between the microsphere and microtubule minus end for the processively moving beads shown in (B). Red lines are the best linear fit for the descending segments of these curves.

(F) Histogram distribution showing the motility rates of the Ska1/Ska2 dimer (n = 25) and the full Ska1 complex (n = 28)-coated microspheres.

(G) A graph showing the average rates of bead motions and the time of bead attachment to the shortening microtubule end. Error bars are SEM.

(H and I) Speculative model for Ska1 complex assembly and function. (H) The bead motions of the Ska1/Ska2 dimer are similar to the Dam1 complex that does not form a ring-like structure, and may be due to the rolling of the beads. The full Ska1 complex moves at a similar rate to the ring-like Dam1 complex. In this model, the Ska1 complex is shown as an oligomeric structure on microtubules. The oligomeric nature of Ska1 is based on the strong cooperativity in microtubule binding, the structures visualized on microtubules by EM, and the movement of the Ska1 along microtubules at a rate that suggests it creates an impediment to microtubule depolymerization. (I) Distinct microtubule coupling activities at the kinetochore include a fibril-like structure such as the Ndc80 complex and an oligomeric assembly such as the Dam1 or Ska1 complex.

contrast, the full Ska1 complex-coated beads displayed a tighter rate distribution (Figures 6F and 6G); on average, these beads moved 30% slower than the shortening rate of a free microtubule. This difference in the rate of the Ska1/Ska2 dimer in the presence and absence of the Rama1 subunit indicates that the full Ska1 complex can support bead attachment to the shortening microtubule end for a substantially longer period of time (Figure 6G). Our data suggest that the complete Ska1 complex forms an oligomeric assembly based on the strong cooperativity in microtubule binding and the assemblies visualized on microtubules by EM. Combining this model of oligomeric Ska1 assemblies with the kinetic bead motility data suggests that the Ska1/Ska2 complex couples microspheres to depolymerizing microtubules similarly to the Dam1 complex not assembled into rings (Figure 6H), whereas the full Ska1 complex functions kinetically similar to a ring-like Dam1 complex (Figure 6H).

DISCUSSION

Here, we have isolated a three subunit Ska1 complex that is an essential component of the human kinetochore and is critical for proper chromosome segregation. This complex directly associates with microtubules as oligomeric assemblies, and it can couple a cargo to microtubule depolymerization. Our work has demonstrated that there are two distinct activities present within the Ska1 complex: a microtubule-binding activity imparted by the Ska1 and, to a lesser extent, Ska2 subunits; and an oligomerization-promoting activity provided by the Rama1 subunit and catalyzed by the microtubule lattice.

Is the Ska1 Complex a Metazoan Functional Counterpart to the Fungal Dam1 Complex?

Previous work has examined the Dam1 complex in budding yeast and fission yeast (Cheeseman et al., 2001b; Janke et al., 2002; Jones et al., 2001; Li et al., 2002; Liu et al., 2005; Sanchez-Perez et al., 2005; Tanaka et al., 2007). These studies have demonstrated a critical role for the Dam1 complex in meditating kinetochore-microtubule attachments and coupling chromosome movement to microtubule depolymerization. The Dam1 complex is particularly well suited to maintain such interactions in budding yeast in which each kinetochore is stably attached to a single microtubule (Grishchuk et al., 2008a). However, despite the important function of the Dam1 complex in fungi, counterparts to the Dam1 complex have not been identified in multicellular organisms. Here, we have identified a three subunit Ska1 complex that is critical for chromosome segregation in human cells. Based on the analyses presented here, there are numerous functional similarities between the Ska1 and Dam1 complexes. However, it is important to note that the Ska1 complex is not a homolog of the Dam1 complex. These complexes show very different subunit composition (the Dam1 complex contains ten subunits, whereas the Ska1 complex contains three subunits), and there is no significant detectable sequence identity between subunits of the Ska1 complex and subunits of the Dam1 complex. Thus, these likely represent evolutionarily distinct complexes. Interestingly, whereas the Dam1 complex is present in fungi, but absent from metazoans, the Ska1 complex is conserved in diverse multicellular organisms, including vertebrates, plants, and nematodes, but is absent from fungi.

Although there is no obvious sequence similarly between the Ska1 and Dam1 complexes, the results presented here demonstrate that there are clear functional and biochemical similarities between these complexes. First, the Ska1 complex and the Dam1 complex both show dual localization to kinetochores and spindle microtubules (Figure 1) (Cheeseman et al., 2001b). Second, the localization of both the Dam1 complex and the Ska1 complex to kinetochores is dependent on the Ndc80 complex and on microtubules (Figure 1) (Hanisch et al., 2006; Janke et al., 2002; Li et al., 2002). Third, overexpression of a microtubule-binding subunit (Ska1 or Dam1) causes defects in microtubule organization (Figure 2) (Hofmann et al., 1998). Fourth, loss of function of the complex results in a checkpoint-dependent mitotic arrest and causes severe chromosome missegregation (Figure 2) (Cheeseman et al., 2001b; Hanisch et al., 2006; Hofmann et al., 1998). Fifth, both complexes bind to microtubules through the acidic C terminus of tubulin with a similar apparent microtubule-binding affinity (Figure 4) (Westermann et al., 2005). Sixth, both complexes form cooperative assemblies on microtubule polymers (Figures 4 and 5) (Miranda et al., 2005; Westermann et al., 2005). And, finally, both the Dam1 complex and the Ska1 complex can processively move a cargo along a microtubule in a depolymerization-coupled manner (Figure 6) (Asbury et al., 2006; Grishchuk et al., 2008b; Westermann et al., 2006). The slow rate of the depolymerization-driven motion of the full Ska1 complex-bound beads is highly reminiscent of the motions of beads coupled to microtubules by the Dam1 ring. Thus, despite the lack of sequence identity, the Ska1 complex has the properties that make it well suited to function as a metazoan counterpart to the Dam1 complex with a critical role at the outer kinetochore to couple chromosome movement with microtubule depolymerization.

Coupling Chromosome Movement to Microtubule Dynamics

A key player in forming kinetochore-microtubule attachments is the KNL-1/Mis12 complex/Ndc80 (KMN) complex network (Cheeseman et al., 2006; Ciferri et al., 2008; DeLuca et al., 2006; Wei et al., 2007). However, it was unclear whether the KMN network is sufficient to maintain interactions with dynamic microtubule polymers. Several recent studies identified additional human proteins that were suggested to function at the kinetochore-microtubule interface, including Bod1 (Porter et al., 2007), Cep57 (Emanuele and Stukenberg, 2007), and Ska1 (Hanisch et al., 2006). Based on data presented here, the Ska1 complex is a key player at the outer kinetochore to mediate chromosome segregation. In contrast, our preliminary studies are not consistent with Cep57 or Bod1 playing a direct role in binding to microtubules at kinetochores (our unpublished data).

There are several possibilities for the specific functions of the Ska1 complex at kinetochores. Despite a lack of sequence similarity to the Dam1 complex, the Ska1 complex may be a true functional counterpart to the Dam1 complex. In this case, like the Dam1 complex, the Ska1 complex would form a microtubule-encircling ring in vivo that couples chromosomes to microtubule depolymerization (Figure 6I). Future work will determine the biophysical properties of the Ska1 complex, including the diffusion properties of Ska1 complex assemblies and its ability to track along the ends of shortening microtubules.

Whereas the Ska1 complex displays many similar properties to the Dam1 complex, it may be optimized for the distinct features of metazoan kinetochores, including different binding partners or a distinct molecular ultrastructure such as the presence of multiple kinetochore-bound microtubules. Recent work suggests that vertebrate cells can facilitate connections with depolymerizing microtubules by using fibril-like connections to microtubule protofilaments (McIntosh et al., 2008). Indeed, the fibril-like Ndc80 complex can couple a microsphere to microtubule depolymerization, but with low efficiency (McIntosh et al., 2008). Ska1 complex oligomers may be adapted to play an integral part in this fibrous mechanism. Whereas numerous fibrils may maintain connections to depolymerizing microtubules and drive chromosome movement, unlike a microtubule-associated oligomer, there is always a possibility that some protofilaments may fail to establish lasting attachments to kinetochore fibrils. Such protofilaments would continue to depolymerize, and the microtubule would lose its integrity and associations with its kinetochore cargo. However, a combination of the fibril-like attachment and an oligomeric complex might mechanically stabilize this structure, thereby helping to ensure the fidelity of motion (diagrammed in Figure 6I). The ability of the Ska1 complex to cooperatively form oligomeric assemblies on the microtubule lattice is pivotal for this proposed function. Future work will examine the connections and relationships between the Ska1 and Ndc80 complexes.

EXPERIMENTAL PROCEDURES

Cell Culture and siRNA Transfection

cDNAs for the human Ska1 complex proteins were obtained as IMAGE clones. Stable clonal cells lines expressing GFP^{LAP}-Ska1, Ska2, and Rama1 were generated as described previously (Cheeseman et al., 2004). Cells were maintained in Dulbecco's modified Eagle's medium (DMEM) supplemented with 10% fetal bovine serum (FBS), penicillin/streptomycin, and L-glutamine (Invitrogen) at 37°C in a humidified atmosphere with 5% CO_2. RNAi experiments were conducted as described previously (Kline et al., 2006). siRNAs against Nuf2 (DeLuca et al., 2002) and pools of four predesigned siRNAs (listed in the 5′ to 3′ direction) against Ska1 (GGACUUACUCGUUAUGUUA, UCAAUGGUGUUCCUUCGUA, UAUAGUGGAAGCUGACAUA, and CCGCUUAACCUAUAAUCAA) and Rama1 (GGAAGAGCCCGUAAUUGUA, GAUCGUACUUCGUUGGUUU, AAUCCAGGCUCAAUGUAA, and CAUCGUAUCCCAAGUUCUA) were obtained from Dharmacon.

Immunofluorescence and Microscopy

Immunofluorescence in human cells was conducted as described previously (Kline et al., 2006). For immunofluorescence against microtubules, DM1α (Sigma) was used at 1:500. For visualization of kinetochore proteins, mouse anti-HEC1 (9G3; Abcam, Cambridge, MA) was used at 1:1000 and human anti-centromere antibodies (ACA; Antibodies, Inc., Davis, CA) were used at 1:100. HeLa cells expressing YFP-CENP-A (Kops et al., 2005) were counterstained with goat anti-GFP (a generous gift of Andres Ladurner) at 1:1000. Affinity-purified rabbit polyclonal antibodies were generated against full-length Ska1, Ska2, and Rama1 as described previously (Desai et al., 2003). Polyclonal antibodies against Ska1, Ska2, and Rama1 were used at 1 μg/ml. Cy2-, Cy3-, and Cy5-conjugated secondary antibodies (Jackson Laboratories) were used at 1:100. DNA was visualized by using 10 μg/ml Hoechst.

Images were acquired on a DeltaVision Core deconvolution microscope (Applied Precision) equipped with a CoolSnap HQ2 CCD camera. A total of 30–40 Z-sections were acquired at 0.2 μm steps by using a 100× 1.3 NA Olympus U-PlanApo objective with 1 × 1 binning. Images were deconvolved by using the DeltaVision software. Equivalent exposure conditions and scaling were used between controls and RNAi-depleted cells.

Protein Purification and Biochemical Assays

GFP^{LAP}-tagged Ska1, Ska2, and Rama1 were isolated from HeLa cells as described previously (Cheeseman and Desai, 2005). Purified proteins were identified by mass spectrometry by using an LTQ XL Ion trap mass spectrometer (Thermo) with MudPIT and SEQUEST software as described previously (see Cantin et al., 2007; Washburn et al., 2001).

The Ska1 complex proteins were induced and isolated essentially as described previously (Cheeseman et al., 2006). For the expression and purification of the recombinant proteins, GST fusions with full-length Ska1, Ska2, and Rama1 were generated in pGEX-6P-1. GST-Ska1 and GST-Ska2 were eluted from the glutathione agarose by the addition of 10 mM glutathione, whereas Rama1 was eluted from this resin by using cleavage with GST-PreScission protease. For coexpression of Ska2 and Ska1-6xHis, these were subcloned into the polycistronic expression system (pET3aTr/pST39) (Tan, 2001). The 6xHis-tagged fusion was eluted from Ni-NTA agarose with 250 mM imidazole. In each case, after elution from the glutathione agarose or Ni-NTA agarose, the protein was concentrated in an Amicon Ultra column with a 30 kDa cutoff and separated on a Superdex 200 size-exclusion column into 25 mM HEPES (pH 7.0), 1 mM EDTA, 150 mM KCl, 1 mM DTT. For the purification of the full Ska1 complex, Ska2/Ska1-6xHis was eluted from the Ni-NTA agarose and bound to GST-Rama1 isolated on gluthione agarose resin. The resin was washed, and the full complex was eluted with GST-PreScission. The complex was then concentrated and fractionated on the Superdex 200 column. Microtubule-binding and -bundling assays with the purified proteins were conducted as described previously (Cheeseman et al., 2006). To determine the binding of the Ska1 complex in the absence of the acidic C terminus of tubulin, GMPCPP-stabilized microtubules were treated with 250 μg/ml type XXIV subtilisin (Sigma) for 60 min at 30°C.

Electron Microscopy

Microtubules decorated with the full Ska1 complex and the Ska1/Ska2 dimer were stained and visualized by using negative-stain electron microscopy (EM) on continuous carbon that had been glow discharged. A total of 4 μl of 1 μM microtubules were applied to the grid for 1 min and briefly washed across with BRB80 buffer. A total of 4 μl of the Ska1 complex at ~0.2 mg/ml was then applied to the microtubule-bound grid for 1 min. The sample was washed with BRB80 to remove unbound protein and then washed and stained twice with 10 μl 2% uranyl acetate. The stained sample was left to sit on the grid for 1 min, then blotted to dry. Images were acquired on a Technai Spirit electron microscope at 120 kV by using a CCD camera.

In Vitro Motility of Protein-Coated Beads

The assays were carried out as described by Grishchuk et al. (2005), and the beads were coated with proteins as by Grishchuk et al. (2008b). Briefly, streptavidin-coated polystyrene beads (Bangs Laboratories, Inc.) were functionalized with saturating amounts of biotinylated anti-6xHis antibodies (Abcam) and then with Ska1/Ska2 dimer or full Ska1 complex proteins containing a 6xHis-tagged Ska1 subunit. Efficient conjugation was confirmed with anti-Ska1 antibodies, followed by fluorescent secondary antibodies. For motility assays, protein-coated beads were washed to remove the unbound protein and then added to an experimental chamber in BRB80 supplemented with 1 mM DTT, 0.5 mg/ml casein, 1 mg/ml BSA, and 2.5–6 nM of the corresponding soluble Ska1 complex proteins. Images were acquired every 0.3–0.4 s with low-light DIC and a Texas red filter, as described by Grishchuk et al. (2008b).

SUPPLEMENTAL DATA

Supplemental Data include one figure and two movies and can be found with this article online at http://www.cell.com/developmental-cell/supplemental/S1534-5807(09)00039-2.

ACKNOWLEDGMENTS

We are grateful to Arshad Desai for his generous support during the early stages of this project; Mary Porter for a kind gift of *Chlamydomonas* axonemes; Paula Grissom for technical assistance; and Angelika Amon, Arshad Desai, Andreas Hochwagen, and Terry Orr-Weaver for critical reading of the manuscript. This work was supported by a Smith Family Foundation Award for Excellence in Biomedical Research to I.M.C. I.M.C. is a Thomas D. and Virginia W. Cabot Career Development Professor of Biology.

Received: November 13, 2008
Revised: January 6, 2009
Accepted: January 23, 2009
Published: March 16, 2009

REFERENCES

Asbury, C.L., Gestaut, D.R., Powers, A.F., Franck, A.D., and Davis, T.N. (2006). The Dam1 kinetochore complex harnesses microtubule dynamics to produce force and movement. Proc. Natl. Acad. Sci. USA *103*, 9873–9878.

Cantin, G.T., Shock, T.R., Park, S.K., Madhani, H.D., and Yates, J.R., 3rd. (2007). Optimizing TiO2-based phosphopeptide enrichment for automated multidimensional liquid chromatography coupled to tandem mass spectrometry. Anal. Chem. *79*, 4666–4673.

Cheeseman, I.M., and Desai, A. (2005). A combined approach for the localization and tandem affinity purification of protein complexes from metazoans. Sci. STKE *2005*, pl1.

Cheeseman, I.M., and Desai, A. (2008). Molecular architecture of the kinetochore-microtubule interface. Nat. Rev. Mol. Cell Biol. *9*, 33–46.

Cheeseman, I.M., Brew, C., Wolyniak, M., Desai, A., Anderson, S., Muster, N., Yates, J.R., Huffaker, T.C., Drubin, D.G., and Barnes, G. (2001a). Implication of a novel multiprotein Dam1p complex in outer kinetochore function. J. Cell Biol. *155*, 1137–1146.

Cheeseman, I.M., Enquist-Newman, M., Müller-Reichert, T., Drubin, D.G., and Barnes, G. (2001b). Mitotic spindle integrity and kinetochore function linked by the Duo1p/Dam1p complex. J. Cell Biol. *152*, 197–212.

Cheeseman, I.M., Niessen, S., Anderson, S., Hyndman, F., Yates, J.R., III, Oegema, K., and Desai, A. (2004). A conserved protein network controls assembly of the outer kinetochore and its ability to sustain tension. Genes Dev. *18*, 2255–2268.

Cheeseman, I.M., Chappie, J.S., Wilson-Kubalek, E.M., and Desai, A. (2006). The Conserved KMN network constitutes the core microtubule-binding site of the kinetochore. Cell *127*, 983–997.

Ciferri, C., Pasqualato, S., Screpanti, E., Varetti, G., Santaguida, S., Dos Reis, G., Maiolica, A., Polka, J., De Luca, J.G., De Wulf, P., et al. (2008). Implications for kinetochore-microtubule attachment from the structure of an engineered Ndc80 complex. Cell *133*, 427–439.

DeLuca, J.G., Moree, B., Hickey, J.M., Kilmartin, J.V., and Salmon, E.D. (2002). hNuf2 inhibition blocks stable kinetochore-microtubule attachment and induces mitotic cell death in HeLa cells. J. Cell Biol. *159*, 549–555.

DeLuca, J.G., Gall, W.E., Ciferri, C., Cimini, D., Musacchio, A., and Salmon, E.D. (2006). Kinetochore microtubule dynamics and attachment stability are regulated by Hec1. Cell *127*, 969–982.

Desai, A., Rybina, S., Muller-Reichert, T., Shevchenko, A., Shevchenko, A., Hyman, A., and Oegema, K. (2003). KNL-1 directs assembly of the microtubule-binding interface of the kinetochore in *C. elegans*. Genes Dev. *17*, 2421–2435.

Emanuele, M.J., and Stukenberg, P.T. (2007). *Xenopus* Cep57 is a novel kinetochore component involved in microtubule attachment. Cell *130*, 893–905.

Grishchuk, E.L., Molodtsov, M.I., Ataullakhanov, F.I., and McIntosh, J.R. (2005). Force production by disassembling microtubules. Nature *438*, 384–388.

Grishchuk, E.L., Efremov, A.K., Volkov, V.A., Spiridonov, I.S., Gudimchuk, N., Westermann, S., Drubin, D., Barnes, G., McIntosh, J.R., and Ataullakhanov, F.I. (2008a). The Dam1 ring binds microtubules strongly enough to be a processive as well as energy-efficient coupler for chromosome motion. Proc. Natl. Acad. Sci. USA *105*, 15423–15428.

Grishchuk, E.L., Spiridonov, I.S., Volkov, V.A., Efremov, A., Westermann, S., Drubin, D., Barnes, G., Ataullakhanov, F.I., and McIntosh, J.R. (2008b). Different assemblies of the DAM1 complex follow shortening microtubules by distinct mechanisms. Proc. Natl. Acad. Sci. USA *105*, 6918–6923.

Hanisch, A., Sillje, H.H., and Nigg, E.A. (2006). Timely anaphase onset requires a novel spindle and kinetochore complex comprising Ska1 and Ska2. EMBO J. *25*, 5504–5515.

Hofmann, C., Cheeseman, I.M., Goode, B.L., McDonald, K.L., Barnes, G., and Drubin, D.G. (1998). *Saccharomyces cerevisiae* Duo1p and Dam1p, novel proteins involved in mitotic spindle function. J. Cell Biol. *143*, 1029–1040.

Janke, C., Ortiz, J., Tanaka, T.U., Lechner, J., and Schiebel, E. (2002). Four new subunits of the Dam1-Duo1 complex reveal novel functions in sister kinetochore biorientation. EMBO J. *21*, 181–193.

Jones, M.H., He, X., Giddings, T.H., and Winey, M. (2001). Yeast Dam1p has a role at the kinetochore in assembly of the mitotic spindle. Proc. Natl. Acad. Sci. USA *98*, 13675–13680.

Kline, S.L., Cheeseman, I.M., Hori, T., Fukagawa, T., and Desai, A. (2006). The human Mis12 complex is required for kinetochore assembly and proper chromosome segregation. J. Cell Biol. *173*, 9–17.

Kops, G.J., Kim, Y., Weaver, B.A., Mao, Y., McLeod, I., Yates, J.R., 3rd, Tagaya, M., and Cleveland, D.W. (2005). ZW10 links mitotic checkpoint signaling to the structural kinetochore. J. Cell Biol. *169*, 49–60.

Li, Y., Bachant, J., Alcasabas, A.A., Wang, Y., Qin, J., and Elledge, S.J. (2002). The mitotic spindle is required for loading of the DASH complex onto the kinetochore. Genes Dev. *16*, 183–197.

Liu, X., McLeod, I., Anderson, S., Yates, J.R., 3rd, and He, X. (2005). Molecular analysis of kinetochore architecture in fission yeast. EMBO J. *24*, 2919–2930.

McIntosh, J.R., Grishchuk, E.L., Morphew, M.K., Efremov, A.K., Zhudenkov, K., Volkov, V.A., Cheeseman, I.M., Desai, A., Mastronarde, D.N., and Ataullakhanov, F.I. (2008). Fibrils connect microtubule tips with kinetochores: a mechanism to couple tubulin dynamics to chromosome motion. Cell *135*, 322–333.

Miranda, J.J., De Wulf, P., Sorger, P.K., and Harrison, S.C. (2005). The yeast DASH complex forms closed rings on microtubules. Nat. Struct. Mol. Biol. *12*, 138–143.

Porter, I.M., McClelland, S.E., Khoudoli, G.A., Hunter, C.J., Andersen, J.S., McAinsh, A.D., Blow, J.J., and Swedlow, J.R. (2007). Bod1, a novel kinetochore protein required for chromosome biorientation. J. Cell Biol. *179*, 187–197.

Sanchez-Perez, I., Renwick, S.J., Crawley, K., Karig, I., Buck, V., Meadows, J.C., Franco-Sanchez, A., Fleig, U., Toda, T., and Millar, J.B. (2005). The DASH complex and Klp5/Klp6 kinesin coordinate bipolar chromosome attachment in fission yeast. EMBO J. *24*, 2931–2943.

Siegel, L.M., and Monty, K.J. (1966). Determination of molecular weights and frictional ratios of proteins in impure systems by use of gel filtration and density gradient centrifugation. Application to crude preparations of sulfite and hydroxylamine reductases. Biochim. Biophys. Acta *112*, 346–362.

Steegmaier, M., Yang, B., Yoo, J.S., Huang, B., Shen, M., Yu, S., Luo, Y., and Scheller, R.H. (1998). Three novel proteins of the syntaxin/SNAP-25 family. J. Biol. Chem. *273*, 34171–34179.

Tan, S. (2001). A modular polycistronic expression system for overexpressing protein complexes in *Escherichia coli*. Protein Expr. Purif. *21*, 224–234.

Tanaka, T.U., and Desai, A. (2008). Kinetochore-microtubule interactions: the means to the end. Curr. Opin. Cell Biol. *20*, 53–63.

Tanaka, K., Kitamura, E., Kitamura, Y., and Tanaka, T.U. (2007). Molecular mechanisms of microtubule-dependent kinetochore transport toward spindle poles. J. Cell Biol. *178*, 269–281.

Washburn, M.P., Wolters, D., and Yates, J.R., 3rd. (2001). Large-scale analysis of the yeast proteome by multidimensional protein identification technology. Nat. Biotechnol. *19*, 242–247.

Wei, R.R., Al-Bassam, J., and Harrison, S.C. (2007). The Ndc80/HEC1 complex is a contact point for kinetochore-microtubule attachment. Nat. Struct. Mol. Biol. *14*, 54–59.

Westermann, S., Avila-Sakar, A., Wang, H.W., Niederstrasser, H., Wong, J., Drubin, D.G., Nogales, E., and Barnes, G. (2005). Formation of a dynamic kinetochore- microtubule interface through assembly of the Dam1 ring complex. Mol. Cell *17*, 277–290.

Westermann, S., Wang, H.W., Avila-Sakar, A., Drubin, D.G., Nogales, E., and Barnes, G. (2006). The Dam1 kinetochore ring complex moves processively on depolymerizing microtubule ends. Nature *440*, 565–569.

Wilson-Kubalek, E.M., Cheeseman, I.M., Yoshioka, C., Desai, A., and Milligan, R.A. (2008). Orientation and structure of the Ndc80 complex on the microtubule lattice. J. Cell Biol. *182*, 1055–1061.